IMAGE COREGISTRATION IN SAR INTERFEROMETRY

Zhengxiao Li [a], James Bethel [b]

[a] ERDAS, Inc. (Leica Geosystems Geospatial Imaging), 5051 Peachtree Corners Circle, Norcross, GA 30092, USA – tonybest@gmail.com

[b] Purdue University, School of Civil Engineering, 550 Stadium Mall Drive, West Lafayette, IN 47907-2051, USA – bethel@purdue.edu

KEY WORDS: SAR Interferometry, Co-registration, Interferometric SAR (InSAR), Matching, Correlation, Interpolation, Synthetic aperture radar (SAR), Geophysics

ABSTRACT:

A critical procedure in Synthetic Aperture Radar (SAR) Interferometric (InSAR) processing was studied: SAR image coregistration. Two pairs of ERS-1/2 SAR tandem data, representing diverse terrain types and different baselines, were used in this research. The commonly used traditional SAR image coregistration algorithms were addressed and tested; the computationally intensive algorithms were examined; the results from those algorithms were compared, through the experiments carried out on real data. The results showed that the magnitude component had better performance compared to complex data for computing cross-correlation function. For fine coregistration, oversampling the cross-correlation function was more efficient than oversampling original SAR images and a factor of 10 was appropriate as the oversampling rate. A particular 4-parameter transformation was sufficient for subpixel coregistration of ERS SAR tandem data. The traditional resampling algorithms, nearest neighbour, bilinear, and cubic convolution, were tested and compared to the computationally intensive sinc interpolators with varied lengths. The most efficient sinc length was not always the longer one. The 2D sinc interpolation with windowing and modulation demonstrated the power of frequency preservation, but no evidence showed that the sinc produced better coherence than the common algorithms. The final InSAR DEM accuracy should be the ultimate standard for evaluating the best coregistration approaches.

1. INTRODUCTION

SAR interferometry requires pixel-to-pixel match between common features in SAR image pairs. Thus coregistration, the alignments of SAR images from two antennas, is an essential step for the accurate determination of phase difference and for noise reduction. SAR images are acquired from about 850 km slant range distance with baseline of approx. 200 m, so there is no visible parallax or disparity between the images. The entire purpose of the coregistration is to align the samples for phase differencing. The imprecise repeat-pass geometry makes coregistration difficult, and the InSAR complex data could facilitate coregistration.

The normal optical image matching traditionally needs only one or two pixel accuracy, which is coarse coregistration for SAR images. The correlation window is used to search for offsets between master and slave images. After this pixel level coregistration, an interferogram may be generated, but it is not adequate for interferometric processing. The phase coregistration accuracy must be higher, so a subpixel level coregistration must be performed.

The subpixel-to-subpixel match, also called fine coregistration, is a must for high precision InSAR results. Either the whole complex image or phase function is up-sampled to 1/8, 1/10, 1/20, or even 1/100 pixel, in order to find the best sub-pixel alignment. One offset is not adequate for resampling the coregistered slave image. First or second order polynomial transformation equations are preferred to fit the conjugate matching points.

The most commonly used method for coregistration is to compute the complex cross correlation function between the two SAR images (Li and Goldstein, 1990). Another approach involves estimating a signal-to-noise ratio (SNR) of the interferogram image (Gabriel and Goldstein, 1988). The average fluctuation function of the interferogram image can be used to adjust the coregistration parameters (Lin et al., 1992).

The capability of computing hardware has advanced significantly in the past decade, while the cost has decreased tremendously. Advanced algorithms can now be used and improved operationally.

In this paper, the commonly used SAR image coregistration algorithms are summarized, from the basic approaches, such as bilinear interpolation, to advanced methods, such as sinc interpolation. Those algorithms were not only discussed theoretically but also examined with real data. The conditions, factors, and characteristics for those algorithms were analyzed and compared broadly. Enhancements to these algorithms were proposed and tested with real data. The experiments also evaluated the theory and simulations in the earlier papers.

2. METHODOLOGY AND ALGORITHM

The typical SAR coregistration procedure consists of 1) coarse coregistration for pixel level accuracy, including searching for coarse image offsets and shifting the slave image; 2) fine coregistration for subpixel accuracy, including searching for subpixel tie points, fitting transformation equations, and resampling the slave image. Coarse coregistration is a process to match two SAR images at up to one or two pixel accuracy. Fine coregistration is a process to find subpixel tie points on two SAR images, to fit transformation equations onto these tie points, and to resample one of these two SAR images based on

the transformation equations. The coregistration performance is usually evaluated by coherence and the accuracy of the final InSAR DEM. Figure 1 is a typical work flow for SAR image coregistration.

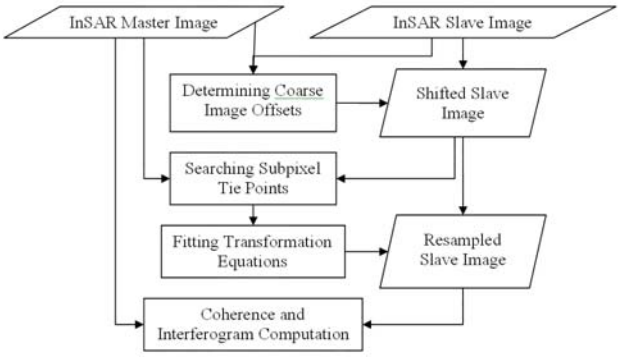

Figure 1 Typical flow chart for SAR image coregistration

2.1 Coarse Coregistration

Coarse coregistration is the step where two SAR images are coregistered at up to one or two pixels accuracy. One of these two SAR images must be assigned as the master (reference) image and another one is the slave (match) image. Through the whole coregistration process, only the slave image will be shifted in coarse coregistration and resampled in fine coregistration. Usually the image located closer to the target of interest is selected as the master image to provide the best geometry. (Leica1, 2007)

Cross-correlation (Li and Goldstein, 1990; Liao et al., 2004) is the most commonly used approach for coarse coregistration. The algorithm is simple to implement, the speed and accuracy are acceptable, and it is not data sensitive and can be applied in automatic InSAR processing easily. Cross-correlation can be calculated in frequency domain for the faster processing.

After all patch pairs with good cross-correlation are finalized, the average peak coordinates are computed and regarded as range and azimuth offsets between two SAR images. The slave SAR image will be shifted by the range and azimuth offsets.

2.2 Fine Coregistration

2.2.1 Searching for Subpixel Tie Points

The first question about this process that one needs to address is how fine the coregistration should be, 1/2, 1/5, 1/8, 1/10, or 1/20 pixel? In 1990, Li and Goldstein found the phase error was about 30 degrees when the signal-to-noise ratio (SNR) was 16 dB for SeaSAT SAR interferometry (Li and Goldstein, 1990). Later, 40 degrees phase random error (equivalent to 20~30 meters vertical DEM error) was commonly utilized for ERS SAR interferometry. Because the phase range for SAR images is always 360 degrees (2π), roughly 1/10 pixel has become widely accepted for fine coregistration (Hanssen and Bamler, 1999; Kwoh et al., 1994; Rufino et al., 1996; Rufino et al., 1998).

Cross-correlation is not only for coarse coregistration, but also a common criterion for fine coregistration. There is disagreement as to the best way of obtaining subpixel offsets. Some researchers oversampled the coarse cross-correlation peaks and looked for the subpixel peaks. Li and Goldstein sought the maximum subpixel peaks by a linear fit 3-point interpolation, achieved the subpixel accuracy of 0.05 pixel (Li and Goldstein, 1990). Other researchers oversampled SAR image patches, computed cross-correlation of the oversampled SAR images and searched for the peaks. Rufino et al. searched for subpixel tie points by oversampling both image subsets by 10 times with a cubic B-spline algorithm (Rufino et al., 1996; Rufino et al., 1998). Kwoh et al. moved one image chip by 0.1 pixels for each cross-correlation computation, which can be considered as equivalent to oversampling images by 10 times for subpixel coregistration (Kwoh et al., 1994).

Using complex data or magnitude only for cross-correlation computation is also an issue for fine coregistration. Complex data containing both magnitude and phase information, could provide more information for cross-correlation computation, but could also introduce phase spectrum noise when the decorrelation is significant. Prati and Rocca used complex data for coregistration (Prati and Rocca, 1990). Kwoh et al. concluded that magnitude only cross-correlation was better than complex cross-correlation for ERS SAR data (Kwoh et al., 1994). Rufino et al. used magnitude only as well (Rufino et al., 1996; Rufino et al., 1998).

2.2.2 Fitting Transformation Equations

After coarse coregistration, the remaining offsets between two SAR images mainly exist in range direction. That is because the parallel baseline component ($B_{||}$) between two platforms varies almost linearly from near range to far range. (Li and Goldstein, 1990). The resulting change of offset is limited to approximate two pixels for ERS SAR images. Very small offsets in the azimuth direction can be detected after coarse coregistration. (Rufino et al., 1996; Rufino et al., 1998)

Thus a number of researchers apply only the following four parameter transformation equations (Eq. (1)) onto subpixel tie points.

$$\begin{aligned} X &= x + ax + c \\ Y &= y + dx + f \end{aligned} \tag{1}$$

(X, Y) are the coordinates of tie points in the slave image, and (x, y) are the coordinates of corresponding points in master image. There is no first order coefficient for y, because most offsets are only proportional to the range pixel location. These equations are sufficient for ERS tandem mode SAR images. They are also employed in commercial software packages, like ASF SAR tools and Leica ERDAS IMAGINE.

If there is more distortion along the y direction, one can use the 6-parameter, first order transformation equations:

$$\begin{cases} X = x + ax + by + c \\ Y = y + dx + ey + f \end{cases} \quad or \quad \begin{cases} X = ax + by + c \\ Y = dx + ey + f \end{cases} \tag{2}$$

Sometimes the 12-parameter second order transformation equations for highly distorted SAR images are applied. The second order equations are more than adequate for ERS tandem mode SAR images. However, in some investigations, even

bicubic polynomial equations for ERS tandem data were used (Rufino et al., 1996; Rufino et al., 1998).

In this research, all these transformation equations (4, 6, and 12 parameters) were tested with real data. Through comparison, the most effective transformation equations were investigated. All polynomial equations are solved by least squares.

2.2.3 Resampling Slave Image

After transformation equations are set up, one can resample the slave image according to the subpixel transformation. Interpolators commonly used for resampling optical images, such as bilinear and cubic convolution, are also used for SAR complex images (Kwoh et al., 1994; Liao et al., 2004).

However, SAR images are complex data, which contain not only intensity information, but also phase information. Each degree error of this phase data is directly related to the InSAR DEM error. Moreover, most SAR images have none-zero Doppler centroid. The interpolation error due to repeated spectrum overlap aliasing and spectrum corner cutoff should be avoided. The interpolator must therefore be selected carefully for resampling SAR images. Hanssen and Bamler investigated the theory and simulation of nearest neighbor, bilinear, four- and six-point cubic convolution, and truncated sinc kernels applied in SAR image resampling. (Hanssen and Bamler, 1999)

In SAR image resampling, the tradeoff between accuracy and computational effort must be considered when selecting interpolation kernels. Hanssen and Bamler (Hanssen and Bamler, 1999) performed both a comprehensive theoretical analysis for these most commonly used interpolators and a simulation study to evaluate these interpolators with coherence and phase error as criteria. The authors listed the following interpolators and their spectra: nearest neighbor, bilinear, four-point cubic convolution, and truncated sinc.

Due to the truncation of the sinc function, a Gibbs phenomenon appears. Gibbs phenomenon is also called ringing artifacts, the oscillations of sinc spectrum near the jump. Usually a windowing filter should have been applied to eliminate the oscillations. Also, SAR images normally have a non-zero Doppler centroid, so the band pass sinc function should have been modulated to work better on SAR images (ESA, 1999).

A band limited continuous signal, if sampled without aliasing, can be reconstructed by convolving with a sampled infinite sinc function. However, an infinite sinc function is not possible and one always has to truncate the sinc kernel. The sinc length S is preferred to be an odd number in the ESA manual (ESA, 1999). A typical truncated discrete sinc function for image resampling could be:

$$\begin{aligned} &F(n) = Sinc[\pi(n+\Delta)], \\ &n = -\frac{(S-1)}{2},...,0,...,\frac{(S-1)}{2} \\ &\Delta \in [-0.5, 0.5) \end{aligned} \tag{3}$$

In Eq. (3), Δ is a fractional number representing the coordinate difference between the nearest original point and the interpolated point.

If the sinc length S is an even number (Hanssen and Bamler, 1999), the sinc function is the same as Eq. (3), but $n = -S/2+1, \ldots, 0, \ldots, S/2$. Δ becomes a fractional number representing the coordinate difference between the nearest original point on the left side and the interpolated point, so Δ belongs to [0, 1).

$$\begin{aligned} &F(n) = Sinc[\pi(n+\Delta)], \\ &n = -\frac{S}{2},...,0,...,\frac{S}{2} \\ &\Delta \in [0,1) \end{aligned} \tag{4}$$

If the original discrete signal is $x(n)$, S is an odd number, and the interpolated point is at $(m-\Delta)$, the value of the interpolated point is

$$x(m-\Delta) = \sum_{k=m-\frac{S-1}{2}}^{k=m+\frac{S-1}{2}} x(k)\,Sinc\left[\pi(k-m+\Delta)\right] \tag{5}$$

A Hann Window $W(n)$ can be added to reduce Gibbs phenomenon.

$$\begin{aligned} &W(n) = \frac{1}{2} + \frac{1}{2}\cos\left[\frac{\pi}{\frac{S}{2}+1}(n+\Delta)\right] \\ &n = -\frac{(S-1)}{2},..., 0,..., \frac{(S-1)}{2} \end{aligned} \tag{6}$$

Not only Hann window, many other windows, such as Kaiser window, can also reduce Gibbs phenomenon.

In order to make the resampled image independent of the length of the sinc, a normalization coefficient A is required for the output image:

$$A = \sum_{k=-\frac{S-1}{2}}^{k=\frac{S-1}{2}} F(k)W(k) \tag{7}$$

SAR images normally have non-zero Doppler centroid, though they are band limited data. The sinc function is a band pass filter, so it is better to modulate the sinc function to fit the SAR image spectrum. The modulation function is:

$$\begin{aligned} &M(n) = e^{-j2\pi f_c[n+\Delta+(S-1)/2]} \\ &f_c = \frac{f_{dc}}{PRF} \\ &n = -\frac{(S-1)}{2},...,0,...,\frac{(S-1)}{2} \end{aligned} \tag{8}$$

f_c is called the central frequency of the SAR image, normalized at [-0.5, 0.5]. f_{dc} is the Doppler Centroid Frequency and PRF is the Pulse Response Frequency of the SAR image.

After windowing, modulation, and normalization, the value of the interpolated point is:

$$x(m-\Delta)=\frac{\sum_{k=m-\frac{S-1}{2}}^{k=m+\frac{S-1}{2}} x(k)F(k-m)W(k-m)M(k-m)}{\sum_{k=m-\frac{S-1}{2}}^{k=m+\frac{S-1}{2}} F(k-m)W(k-m)} \quad (9)$$

Eq. (9) is only for one dimensional (1D) data, or one row/column of a SAR image. To resample the 2D SAR image, one can apply Eq. (9) separately: range interpolation and azimuth interpolation. If the sinc length is *S*, (*S+1*) 1D interpolation computations are needed, *S* of which are performed along the range (rows) around the interpolated point and the (*S+1*)th 1D interpolation computation is for interpolating the *S* interpolated range values along azimuth direction (columns). One can find more explanation about the above equations in the ESA manual (ESA, 1999).

The non-zero Doppler centroid for ERS SAR images is only along the azimuth direction. No modulation is needed for range interpolation, and only azimuth interpolation requires modulation.

In this research, two 1D sinc interpolations were not employed separately, but one 2D sinc interpolation simultaneously. The 2D separable sinc function is applied:

$$F(n_x,n_y)=Sinc[\pi(n_x+\Delta_x)]Sinc[\pi(n_y+\Delta_y)],$$
$$n_x=-\frac{(S_x-1)}{2},\ldots,0,\ldots,\frac{(S_x-1)}{2} \qquad n_y=-\frac{(S_y-1)}{2},\ldots,0,\ldots,\frac{(S_y-1)}{2} \quad (10)$$
$$\Delta_x,\Delta_y\in[-0.5,0.5)$$

The sinc length S can also be different for range and azimuth direction. All the other additional equations also need modifying to 2D cases accordingly, except Eq. (8), where the modulation is still applied one dimensionally, i.e. in the azimuth direction. The computational effort for 2D sinc interpolation is one 1D interpolation less than two separate 1D sinc interpolations.

The sinc length *S* is an odd number in Eq. (10). It can also be even number too. Hanssen and Bamler simulated sinc interpolation with sinc length of even number (Hanssen and Bamler, 1999). The paper from the European Space Agency proposed a sinc length of odd number. In this research, sinc lengths of both even and odd numbers are applied.

These algorithms are applied and discussed with real ERS SAR data. The advantage and disadvantage of using sinc interpolation are discussed in this investigation.

2.2.4 Coregistration Evaluation

Most InSAR researches apply the coherence image to evaluate the performance of SAR image coregistration. In this study, the average of the whole coherence image is used as criteria, to evaluate the coregistration results from the above coregistration functions and algorithms.

The final InSAR DEM is certainly another good criterion for estimating SAR image coregistration. The better coregistration performance should result in a higher InSAR DEM accuracy, i.e. a lower InSAR DEM error. The Root Mean Square Error (RMSE) between the InSAR DEM and the reference DEM is computed to evaluate InSAR DEM accuracy, in order to evaluate SAR image coregistration.

3. DATA, TOOLS AND EXPERIMENT

3.1 Data and Tools

As the SAR data, two pairs of ERS-1/2 tandem mode single-look complex images were used. Those ERS SAR data were granted through project 3889 by ESA.

The first pair consists of one ERS-1 image acquired on November 8, 1995, and one ERS-2 image acquired on November 9, 1995. The rough perpendicular baseline between them is 236 meters. This pair covers about 10 counties in northern Indiana, USA. This area is a flat area.

The second pair consists of one ERS-1 image acquired on October 20, 1995, and one ERS-2 image acquired on October 21, 1995. The rough perpendicular baseline between them is 145 meters. This pair covers about 10 counties in southern Indiana, USA, a more hilly area.

The reference DEM was produced from the "Indiana 2005 State-wide Orthophotography Project", which includes a high resolution DEM (Orthophoto DEM). The DEM has 5-foot (~1.5m) post spacing and 6-foot (~1.8m) vertical accuracy at 95% confidence level.

Matlab is the main tool that was employed for SAR image coregistration and coherence computation. Leica ERDAS IMAGINE was used for generating a final InSAR DEM.

3.2 Experiment

The experiments for SAR image coregistration were also motivated by the rapidly improving hardware capabilities, while it was not easy to implement these computationally intensive algorithms before. These SAR image coregistration algorithms can now be evaluated in a different computational environment.
The main experiment is to examine and compare interpolators, including nearest neighbor, bilinear, cubic convolution and sinc function, implement and verify sinc add-ons for SAR image coregistration, using ERS SAR data.

For coarse coregistration, complex and magnitude only were tested and compared for cross-correlation computation. The magnitude only should be good enough for coarse coregistration.

More experiments were performed for fine coregistration. To obtain subpixel cross-correlation peak, both oversampling cross-correlation function and oversampling SAR images were tested and compared. Also 1/10 pixel accuracy requirement was examined by comparing oversampling cross-correlation function by the factors of 10 times and 100 times.

Four parameter transformation equations, which are sufficient, were mostly agreed. Six and 12 parameter transformation equations were tested as well, and it is interesting to see how much the coregistration can be improved using these higher ordered transformation equations, considering computation effort is not the issue as it was in the 1990's.

The nearest neighbor, bilinear, cubic convolution, and sinc interpolators for resampling the slave image were all investigated. The 2D sinc lengths include both odd and even numbers, varying from 2 to 8. Both sinc add-ons: modulation and Hann window were demonstrated and applied.

The coregistration performance was evaluated against the coherence of the two coregistered SAR images and the accuracy of the InSAR DEM. Our own program was developed to compute coherence. The results were compared to the coherence as computed by commercial software. The InSAR DEM was generated through commercial software.

4. RESULTS AND ANALYSIS

The average coherences computed from the master SAR image and the resampled slave SAR images were recorded into tables. The coherence comparison and analysis were conducted side by side.

4.1 Coherences of Original and Coarse Coregistered SAR Images

Searching Subpixel Tie Points and Offsets			# of Pars	Interpolator	Coherence	
Method	Rate	Kernel			North	South
Original	N/A	N/A	0	N/A	0.2554	0.2542
Coarse	N/A	N/A	2	N/A	0.3181	0.3517

Table 1 Coherences of coarse coregistered SAR images

Table 1 contains the coherences out of the original SAR images and coarse coregistered SAR images. If the coherence image is computed from the original master and slave images, the average coherence is 0.2554 for northern Indiana and 0.2542 for southern Indiana. After the slave SAR image was shifted based on coarse coregistration, the average coherence became 0.3181 for northern Indiana and 0.3517 for southern Indiana, a little higher than original SAR images.

4.2 Coherences of Fine Coregistered SAR Images

More factors were examined in fine coregistration for coherence evaluation. First, the approach of oversampling cross-correlation function peak was tested. The oversampling rate was 10. The oversampling kernel was Spline. 4-parameter transformation equations were used. The interpolators included Nearest, Bilinear, Cubic, and Sinc with the lengths from 2 to 8. Modulation was applied to all sinc interpolators.

Searching Subpixel Tie Points and Offsets			# of Pars	Interpolator	Coherence	
Method	Rate	Kernel			North	South
Fit Peak	10	Spline	4	Nearest	0.4297	0.3980
Fit Peak	10	Spline	4	Bilinear	0.4390	0.4596
Fit Peak	10	Spline	4	Cubic	0.4450	0.4461
Fit Peak	10	Spline	4	Sinc2x2	0.4482	0.4177
Fit Peak	10	Spline	4	Sinc3x3	0.4500	0.4201
Fit Peak	10	Spline	4	Sinc4x4	0.4507	0.4217
Fit Peak	10	Spline	4	Sinc5x5	0.4506	0.4218
Fit Peak	10	Spline	4	Sinc6x6	0.4500	0.4213
Fit Peak	10	Spline	4	Sinc7x7	0.4499	0.4213
Fit Peak	10	Spline	4	Sinc8x8	0.4498	0.4211

Table 2 Coherences of oversampling cross-correlation function

After fine coregistration, the coherence increased significantly, even with only nearest neighbor interpolator. The coherence of nearest neighbor is 0.4297 for northern Indiana, much better than the coherence out of coarse coregistration (0.3181). The coherence of nearest neighbor is 0.3980 for southern Indiana, also better than the coherence obtained from coarse coregistration (0.3517). Bilinear yields higher coherence than nearest neighbor for both northern and southern Indiana (0.4390>0.4297 and 0.4596>0.3980). Cubic yields slightly higher coherence than bilinear (0.4450>0.4390) for northern Indiana, but slightly lower coherence than bilinear (0.4461<0.4596) for southern Indiana, so there is not much difference in performance between bilinear and cubic in interpolation.

Theoretically, sinc interpolation should have higher coherence than cubic, bilinear, and nearest neighbor methods; and the longer sinc length should have the higher coherence, but those are not always true. For northern Indiana, all sinc interpolations, even the shortest one, 2-point sinc (0.4482), have higher coherence than cubic and bilinear. The longer length has slightly higher coherence. After Sinc4x4 (0.4507), the coherence is reduced as the sinc length is increased, i.e. sinc4x4 seems to be the best interpolator in this table. If sinc length is longer than 8, the coherence starts to fluctuate, although the overall trend is rising. For southern Indiana, the coherences of bilinear (0.4596) and cubic (0.4461) interpolation are significantly higher than all sinc interpolation with bilinear providing the best results. The trend of sinc interpolation is the same as northern Indiana, though the length of the highest sinc coherence is 5.

Table 3 shows the comparison between oversampling the cross-correlation function by 10 times and by 100 times.

Searching Subpixel Tie Points and Offsets			# of Pars	Interpolator	Coherence	
Method	Rate	Kernel			North	South
Fit Peak	10	Spline	4	Sinc4x4	0.4507	0.4217
Fit Peak	100	Spline	4	Sinc4x4	0.4507	0.4217

Table 3 Coherences of different oversampling rates

100 times oversampling rate does not have higher coherence than 10 times oversampling rate. The results confirm the average random phase error could be much bigger than 1/100 of a wavelength and the higher oversampling rate may not benefit significantly.

Table 4 is the comparison among different number of parameters.

Searching Subpixel Tie Points and Offsets			# of Pars	Interpolator	Coherence	
Method	Rate	Kernel			North	South
Fit Peak	10	Spline	4	Sinc4x4	0.4507	0.4217
Fit Peak	10	Spline	6	Sinc4x4	0.4514	0.4217
Fit Peak	10	Spline	12	Sinc4x4	0.4511	0.4218

Table 4 Coherences of different number of parameters

From Table 4, one can find the number of parameters has no significant effect on the coherence. 4-parameter has been sufficient. 6 parameter transformation equations can model the small deformation with respect to azimuth pixels. The 2nd ranked 12 parameter transformation equations could model more distortion for SAR images, although that is not necessary for this ERS SAR data.

Table 5 shows the coherences of different oversampling methods: oversampling cross-correlation function vs. oversampling SAR images.

Searching Subpixel Tie Points and Offsets			# of Pars	Interpolator	Coherence	
Method	Rate	Kernel			North	South
Fit Peak	10	Spline	6	Sinc4x4	0.4514	0.4217
Up SAR	10	Sinc40	6	Sinc4x4	0.4509	0.4217

Table 5 Coherences of different oversampling methods

Oversampling the SAR image patches did not produce higher coherence than oversampling the cross-correlation function. Oversampling SAR images is also slower than oversampling the cross-correlation function.

The coherence for these two pairs is between 0.4 and 0.5, which seems a little low. The other pairs could have higher coherence, depending on the SAR data properties.

4.3 InSAR DEM Evaluation

Due to the inaccurate orbit and baseline information, InSAR processing without accurate ground control points could result large error in the DEM. By looking at northern Indiana in Table 6, one can find the InSAR DEM of bilinear has slightly smaller DEM error than sinc interpolator, although sinc interpolator has the higher coherence. It is reverse for southern Indiana data: sinc interpolation has the lower coherence, while its InSAR DEM has much higher accuracy.

Searching Subpixel Tie Points and Offsets			# of Pars	Interpolator	InSAR DEM RMSE (Meters)	
Method	Rate	Kernel			North	South
Fit Peak	10	Spline	6	Bilinear	220.64	129.16
Fit Peak	10	Spline	6	Sinc4x4	221.80	65.40

Table 6 InSAR DEM RMSE

5. CONCLUSION

Computing cross-correlation with magnitude only is adequate for both coarse and fine coregistration of ERS SAR data with medium baseline, regardless of whatever terrain is: flat or hilly area. Oversampling the cross-correlation function is more efficient than oversampling SAR images for fine coregistration. The experiments verified oversampling by a factor of 10, and concluded that a particular 4-parameter transformation was sufficient for subpixel coregistration of ERS SAR tandem data.

The widely used resampling algorithms: nearest neighbor, bilinear, and cubic convolution, were tested with those ERS SAR tandem data and were compared to the computationally intensive sinc interpolators with varied lengths. The longer sinc interpolator produced a fluctuating but rising coherence. The 2D sinc interpolation with windowing and modulation exhibited the power of preserving the frequency spectrum, though no evidence showed the sinc interpolator to have better coherence than bilinear or cubic convolution.

This study indicates there may not be a best interpolator for resampling SAR images for all situations. The resampling preference can be affected by terrain type, SAR data type and quality. Coherence is not always a good criterion for estimating the resampling. It is a good indicator for evaluating coregistration within a single image. A higher coherence area indicates a better coregistration location, but coherence may not be a good indicator for comparing coregistration performance of different data sets, or different interpolators. The accuracy of the final InSAR DEM should be the ultimate standard for evaluating coregistration and the whole InSAR processing.

REFERENCES

ESA, E., 1999. Image Interpolation. Nuava Telespazio(3): 93.

Gabriel, A.K. and Goldstein, R.M., 1988. Crossed orbit interferometry: Theory and experimental results from SIR-B. International Journal of Remote Sensing, 9(5): 857-872.

Hanssen, R. and Bamler, R., 1999. Evaluation of interpolation kernels for SAR interferometry. Geoscience and Remote Sensing, IEEE Transactions on, 37(1): 318-321.

Kwoh, L.K., Chang, E.C., Heng, W.C.A. and Hock, L., 1994. DTM generation from 35-day repeat pass ERS-1 interferometry, Geoscience and Remote Sensing Symposium, 1994. IGARSS '94. Surface and Atmospheric Remote Sensing: Technologies, Data Analysis and Interpretation., International, pp. 2288-2290 vol.4.

Leica1, 2007. Introduction to Radar Data. Leica ERDAS IMAGINE Online Documentation, 9.1.

Li, F.K. and Goldstein, R.M., 1990. Studies of multibaseline spaceborne interferometric synthetic aperture radars. Geoscience and Remote Sensing, IEEE Transactions on, 28(1): 88-97.

Liao, M., Lin, H. and Zhang, Z., 2004. Automatic Registration of InSAR Data Based on Least-Square Matching and Multi-Step Strategy. Photogrammetric Engineering & Remote Sensing, 70(10).

Lin, Q., Vesecky, J.F. and Zebker, H.A., 1992. New approaches in interferometric SAR data processing. Geoscience and Remote Sensing, IEEE Transactions on, 30(3): 560-567.

Prati, C. and Rocca, F., 1990. Limits to the resolution of elevation maps from stereo SAR images. International Journal of Remote Sensing, 11(12): 2215-2235.

Rufino, G., Moccia, A. and Esposito, S., 1996. DEM generation by means of ERS tandem data Proceedings of the Fringe '96 Workshop ERS SAR, Zurich, Switzerland.

Rufino, G., Moccia, A. and Esposito, S., 1998. DEM generation by means of ERS tandem data. Geoscience and Remote Sensing, IEEE Transactions on, 36(6): 1905-1912.

ACKNOWLEDGMENTS

ERS data were offered by the European Space Agency. Indiana high resolution DEM data were provided by [2005 Indiana Orthophotography (IndianaMap Framework Data www.indianamap.org)].